OncoTargets and Therapy

Dovepress
open access to scientific and medical research

Open Access Full Text Article

ORIGINAL RESEARCH

Hsa_circ_0006916 Knockdown Represses the Development of Hepatocellular Carcinoma via Modulating miR-599/SRSF2 Axis

This article was published in the following Dove Press journal:
OncoTargets and Therapy

Zhixiang Zhu
Songhe Shen
Sen Zhao
Zhixue Wang

Image Center, The First Affiliated Hospital of Henan University, Kaifeng, Henan 475001, People's Republic of China

Background: The aberrantly expressed circular RNAs (circRNAs) are implicated in the progression of hepatocellular carcinoma (HCC). circRNA hsa_circ_0006916 (circ_0006916) is dysregulated in HCC, but the function and mechanism of this circRNA in HCC development remain uncertain.

Methods: Thirty paired HCC and normal tissues were collected. circ_0006916, microRNA (miR)-599 and serine/arginine rich splicing factor 2 (*SRSF2*) abundances were examined via quantitative reverse transcription polymerase chain reaction or Western blot. Cell viability, colony ability, migration, invasion, cell cycle and apoptosis were tested via cell counting kit-8, colony formation, wound healing analysis, transwell analysis, and flow cytometry. The interaction between miR-599 and circ_0006916 or *SRSF2* was analyzed via dual-luciferase reporter and RNA immunoprecipitation analyses. The function of circ_0006916 on cell growth in vivo was analyzed via xenograft model.

Results: circ_0006916 expression was increased in HCC tissues and cell lines. circ_0006916 knockdown reduced cell viability, colony formation, migration and invasion and caused cell cycle arrest and apoptosis. miR-599 was targeted via circ_0006916, and miR-599 knockdown reversed the influence of circ_0006916 silence on HCC progression. *SRSF2* was targeted via miR-599, and miR-599 overexpression suppressed cell viability, colony formation, migration and invasion and promoted cell cycle arrest and apoptosis via decreasing *SRSF2*. circ_0006916 could regulate *SRSF2* expression via miR-599. circ_0006916 knockdown decreased HCC cell growth in the xenograft model.

Conclusion: circ_0006916 knockdown represses the progression of HCC via regulating miR-599 and *SRSF2*.

Keywords: hepatocellular carcinoma, circ_0006916, miR-599, SRSF2

Introduction

Hepatocellular carcinoma (HCC) is a frequent medical problem ranked as a leading cause of cancer death.[1] Great improvement has gained on understanding the risk, prevention and management of HCC.[2] The surgical resection is a primary option for HCC treatment, but about 70% of patients develop the recurrent cancer with poor outcomes.[3] Thus, it's necessary to find new strategies for the treatment of HCC.

The noncoding RNAs have important roles in the development, pathogenesis and treatment of HCC.[4] Circular RNAs (circRNAs) are a group of highly conserved and stable noncoding RNAs without 5′ and 3′ ends, which are dysregulated and exhibit multiple functions in HCC.[5] CircRNAs can communicate

Correspondence: Zhixue Wang
Image Center, The First Affiliated Hospital of Henan University, 357 Ximen Street, Kaifeng, Henan 475001, People's Republic of China
Tel +86-37122736795
Email hdyfywzx@163.com

submit your manuscript | www.dovepress.com
DovePress
http://doi.org/10.2147/OTT.S267471

with mRNAs via sponging microRNAs (miRNAs) to participate in the development of HCC.[6] For instance, circRNA hsa_circ_0056836 can promote HCC cell migration, proliferation and invasion via regulating miR-766-3p and Fos-related antigen 2 (*FOSL2*).[7] Moreover, hsa_circ_0000092 contributes to the proliferation, migration, invasion and angiogenesis of HCC cells via modulating miR-338-3p and hematological and neurological expressed 1 (*HN1*).[8] In addition, there are some circRNAs playing an anti-cancer role in HCC, such as hsa_circ_0070269 and circRNA-5692.[9,10] Homer scaffolding protein 1 (*HOMER1*) is an important gene significantly associated with the poor survival of HCC patients.[11] The circRNA hsa_circ_0006916 (circ_0006916), derived from *HOMER1*, can repress cell proliferation and promote apoptosis in lung cancer cells.[12] Additionally, emerging evidence suggests that circ_0006916 knockdown mitigates methamphetamine (*METH*)-induced neuronal damage.[13] More importantly, a previous report shows that circ_0006916 expression is enhanced in HCC tissues when compared to non-tumor tissues.[14] Furthermore, circ_0006916 can promote HCC cell proliferation, migration and invasion via modulating miR-1322/C-X-C motif chemokine ligand 6 (*CXCL6*) axis.[15] Nevertheless, the mechanism addressed by circ_0006916 is complex, and additional regulatory network of circ_0006916 is expected to be explored.

miRNAs with ~23 nucleotides control mRNA's abundance via binding to their 3′UTR, thus being relevant to HCC development.[16] miR-599 usually functions as a tumor suppressor via repressing the malignant growth and metastasis of human cancers, such as esophageal carcinoma and gastric cancer.[17,18] More importantly, miR-599 could target *MYC* to restrain cell proliferation, migration and invasion in HCC.[19] Serine/arginine rich splicing factor 2 (*SRSF2*) is highly expressed in HCC and is related to the poor prognosis of patients.[20] Moreover, *SRSF2* can facilitate cell proliferation and tumorigenic potential via regulating cancer-associated splice variants in HCC.[21] The bioinformatic analysis predicts that circ_0006916 and *SRSF2* can bind to miR-599. Hence, we hypothesize that circ_0006916 may target *SRSF2* via regulating miR-599 to participate in HCC development.

In this research, we detected circ_0006916 expression in HCC tissues and cell lines. Moreover, we assessed the function of circ_0006916 on HCC development in vitro and in vivo. Additionally, we analyzed the interaction network of circ_0006916/miR-599/*SRSF2*.

Patients and Methods

Patients and Tissue Collection

Thirty HCC patients who underwent surgery were enrolled from the First Affiliated Hospital of Henan University. They all did not receive any other therapy before surgery. HCC tumor tissues and adjacent normal liver tissues were harvested and maintained at −80°C. All patients provided the written informed consent. This research was permitted via the ethics committee of the First Affiliated Hospital of Henan University, and conducted in line with the Helsinki Declaration.

Cell Culture

Human HCC cell lines (HuH-7 and SNU-387 cells) were purchased from Procell (Wuhan, China) and grew in DMEM (Thermo Fisher, Waltham, MA, USA) plus 10% fetal bovine serum (Gibco, Gran Island, NY, USA) and 1% penicillin/streptomycin (Beyotime, Shanghai, China). The normal liver cell line (THLE-2 cells) was provided via American Type Culture Collection (Manassas, VA, USA) and cultured in BEGM (Lonza/Clonetics Corporation, Walkersville, MD, USA) without gentamycin/amphotericin and epinephrine, but with additional 5 ng/mL epidermal growth factor, 70 ng/mL phosphoethanolamine, and 10% fetal bovine serum. All cells were incubated at 37°C and 5% CO_2.

Quantitative Reverse Transcription Polymerase Chain Reaction (qRT-PCR)

The RNA was extracted using Trizol reagent (Thermo Fisher) following the instructions as previously reported.[22] The RNA with OD260/280 ratio at 1.8~2.0 was used for cDNA generation using the specific reverse transcription kit (Fulengen, Guangzhou, China). Next, the qRT-PCR was performed using the mixture of the generated cDNA, SYBR (Solarbio, Beijing, China) and specific primers (Genscript, Nanjing, China) on an Applied Biosystems 7500 system (Thermo Fisher). The primers were listed as: circ_0006916 (sense, 5′-TCAACGGG ACAGATGATGAA-3′; antisense, 5′-TGTGTTTGGGTCA ATTTGGA-3′), *HOMER1* (sense, 5′-GGCTGCACCTTTA AATTCCC-3′; antisense, 5′-TCCATGTCGCTTCAAGTC CA-3′), *SRSF2* (sense, 5′-CGGTCTCCAGATCTCGTTC G-3′; antisense, 5′-GGTGAGTAACCTCCGAGCAG-3′),

and miR-599 (sense, 5′-GTTGTGTCAGTTTATCAAAC-3′; antisense, 5′-CTCCATATCGCACTTTAATCTCTAACT-3′). U6 (sense, 5′-AATTGGAACGATACAGAGAAGATTAGC-3′; antisense, 5′-TATGGAACGCTTCACGAATTTG-3′), or *GAPDH* (sense, 5′-GAATGGGCAGCCGTTAGGAA-3′; antisense, 5′-AAAAGCATCACCCGGAGGAG-3′) was used as a reference. Relative RNA abundance was calculated by $2^{-\Delta\Delta Ct}$ method.[23]

Detection of circRNA Stability

RNase R (a 3′ to 5′ exonuclease) and Actinomycin D (a transcription inhibitor) were applied to analyze the stability of circ_0006916 as previous reports.[24,25] For RNase R assay, the extracted RNA was treated with 3 U/μg of RNase R (GeneSeed, Guangzhou, China) for 30 min at 37°C, and then the abundances of circ_0006916 and the linear *HOMER1* were detected via qRT-PCR. For Actinomycin D assay, cells were stimulated via 2 μg/mL of Actinomycin D (Amyjet, Wuhan, China) for 24 h, and then the RNA was isolated for the detection of circ_0006916 and the linear HOMER1 expression. The untreated group was regarded as the mock group.

Vector and Oligonucleotide Construction and Cell Transfection

SRSF2 overexpression vector (pc-SRSF2) was constructed via inserting the full-length sequence of *SRSF2* into pcDNA3.1 vector (Thermo Fisher) by endonuclease sites Nhe I and Xho I, with the empty vector as negative control (pc-NC). The siRNA for circ_0006916 (si-circ_0006916, 5′-UUCACAUAGGGAACAACCUAU-3′), negative control of siRNA (si-NC) (5′-UUAAGACAUUGUCUGUCCGCCTT-3′), miR-599 mimic (5′-GUCUGUCAGUUUAUCAAAC-3′), negative control of mimic (mimic NC, 5′-UUCUCCGAACGUGUCACGUUU-3′), miR-599 inhibitor (5′-GUUUGAUAAACUGACAGAAC-3′), and negative control of inhibitor (inhibitor NC, 5′-UGAGCUGCAUAGAGUAGUGCUUA-3′) were formed via GenePharma (Shanghai, China). Huh7 and SNU-387 cells were transfected with the constructed vectors or oligonucleotides by Lipofectamine 3000 (Thermo Fisher) for 24 h.

Cell Counting Kit-8 (CCK8)

Cell viability was analyzed via CCK8. 1×10^4 Huh7 and SNU-387 cells were added into 96-well plates, and grown for 72 h. Next, 10 μL of CCK8 solution (Glpbio, Montclair, CA, USA) was added, and incubated with cells for 2 h. The absorbance was examined through a microplate reader (Bio-Rad, Hercules, CA, USA) with a wavelength of 450 nm. Relative cell viability was normalized to the control group.

Colony Formation Analysis

1×10^3 Huh7 and SNU-387 cells were seeded into the 6-well plates, and then cultured for 10 days. Subsequently, cells were fixed and dyed with 0.5% crystal violet (Beyotime). The colony formation was captured and the numbers were counted.

Wound Healing Analysis

The mobility of Huh7 and SNU-387 cells was assessed via wound healing analysis. 2×10^5 Huh7 and SNU-387 cells were added to 12-well plates, and incubated until reaching ~90% confluence. A straight wound was caused via a 10-μL sterile pipette tip. Next, cells were cultured for 24 h, and the width of wound was measured under a microscope (Nikon, Tokyo, Japan).

Transwell Analysis

The migrated and invasive abilities of cells were analyzed via transwell analysis using transwell chamber (BD, Franklin Lakes, NJ, USA). 5×10^5 Huh7 and SNU-387 cells in serum-free medium were added into the upper chamber precoated with 100 μL of Matrigel (Solarbio) for invasion assay, and 1×10^5 cells in non-serum medium were added to the upper chambers without Matrigel for migration assay. 600 μL of medium with 10% serum was added into the lower chambers. Following culture for 24 h, cells were dyed with 0.5% crystal violet, followed by observation under a microscope (magnification ×100) with 3 randomly selected fields.

Flow Cytometry

Cell cycle distribution and apoptosis were investigated via flow cytometry. For cell cycle detection, Huh7 and SNU-387 cells were incubated in 12-well plates for 72 h, and then cells were fixed with 70% ethanol, and interacted with 1 mg/mL of RNase and 50 μg/mL of propidium iodide (PI) for 30 min. 1×10^4 Huh7 and SNU-387 cells were examined via a flow cytometer (Agilent, Hangzhou, China), and the proportion of cells at G0/G1, S or G2/M phase was tested via ModFit software (Verity Software House, Topsham, ME, USA).

Cell apoptosis was tested with Annexin V-FITC apoptosis kit (Thermo Fisher). 2×10^5 Huh7 and SNU-387

cells were added in 6-well plates and cultured for 72 h. Next, cells were incubated with Annexin V-FITC binding buffer, and then dyed with Annexin V-FITC and PI, followed via the detection with a flow cytometer. The apoptotic rate was displayed as a percentage of cells in the upper and lower right quadrants.

Dual-Luciferase Reporter and RNA Immunoprecipitation (RIP) Analyses

The targets of circ_0006916 were predicted via CircInteractome (http://circinteractome.nia.nih.gov/),[26] and the targets of miR-599 were predicted by starBase (http://starbase.sysu.edu.cn/).[27] The dual-luciferase reporter and RIP analyses were carried out to explore the target correlation of miR-599 and circ_0006916 or *SRSF2*. In brief, the wild-type (circ_0006916 WT or SRSF2-3′UTR WT) or mutant luciferase reporter vectors (circ_0006916 MUT or SRSF2-3′UTR MUT) were generated via inserting the corresponding sequence containing wild-type or mutant miR-599 complementary sites in luciferase gene downstream in PGL3-Control vectors (Promega, Madison, WI, USA) via endonuclease site Xba I. These constructed vectors, control vectors and miR-599 mimic or miRNA NC were transfected into Huh7 and SNU-387 cells for 24 h. The luciferase activity was measured via a dual-luciferase analysis kit (Promega) and Glomax 20/20 Luminometer (Promega).

RIP analysis was conducted with a Magna RIP kit (Sigma, St. Louis, MO, USA). 1×10^7 Huh7 and SNU-387 cells were lysed and interacted with magnetic beads conjugated via anti-Ago2 for 4 h. Next, the RNA enriched on the beads was extracted and used for the detection of circ_0006916, miR-599 and SRSF2 levels. IgG was employed as a negative control, and Input functioned as a positive control.

Western Blot

Cells or tissues were lysed in RIPA buffer (Solarbio) for the collection of total protein, and the protein concentration was examined via a BCA kit (Solarbio). The protein samples (30 μg) were loaded on SDS-PAGE and transferred to nitrocellulose membranes (Bio-Rad). Five percent bovine serum albumin (Solarbio) was used to block the membranes. Next, the membranes were incubated with Abcam antibody (Cambridge, MA, USA) against SRSF2 (ab28428, 1:3000 dilution) overnight and the IgG conjugated via HRP (ab205718, 1:10,000 dilution) for 2 h. GAPDH (ab22555, 1:5000 dilution) functioned as a loading reference. Following exposing to ECL reagent (Abcam), the visualized blots were tested via Image Lab software (Bio-Rad).

Xenograft Experiment

The lentiviral vectors carried shRNA for circ_0006916 (sh-circ_0006916) or negative control (sh-NC) were generated via GenePharma, and transfected into SNU-387 cells. Male BALB/c nude mice (5-week-old) were provided via Charles River (Beijing, China) and arbitrarily divided into sh-circ_0006916 and sh-NC groups (n=6/group). In sh-circ_0006916 group, mice were subcutaneously injected with 5×10^6 SNU-387 cells with stable transfection of sh-circ_0006916. In sh-NC group, mice were subcutaneously injected with 5×10^6 SNU-387 cells with stable transfection of sh-NC. The tumor size was detected every 7 days, and volume was calculated via 0.5 × length × width^2. After 28 days, mice were euthanized via 3% isoflurane. Tumor tissues were harvested and weighed. Next, the expression of circ_0006916, miR-599 and SRSF2 in tumor tissues was detected via qRT-PCR or Western blot. This experiment was approved via the Animal Ethical Committee of the First Affiliated Hospital of Henan University, and performed in line with the National Institutes of Health.

Statistical Analysis

Four replicates were conducted in vitro, and the experiment was repeated 3 times, unless otherwise indicated. The data were reported as mean ± SD, and compared via Student's *t*-test or ANOVA with Tukey's test via GraphPad Prism 7 (GraphPad Inc., La Jolla, CA, USA). The linear correlation of gene expression in HCC tissues was assessed via Pearson test. The difference was considered as significant at $P<0.05$.

Results

circ_0006916 Expression is Enhanced in HCC

To detect the expression change of circ_0006916 in HCC, 30 paired tumor and normal tissues were collected. As exhibited in Figure 1A, circ_0006916 abundance was higher in HCC tissues than normal samples. Furthermore, circ_0006916 level was evidently elevated in HCC cell lines (Huh7 and SNU-387 cells) compared with normal liver cell line (THLE-2 cells) (Figure 1B). To test the

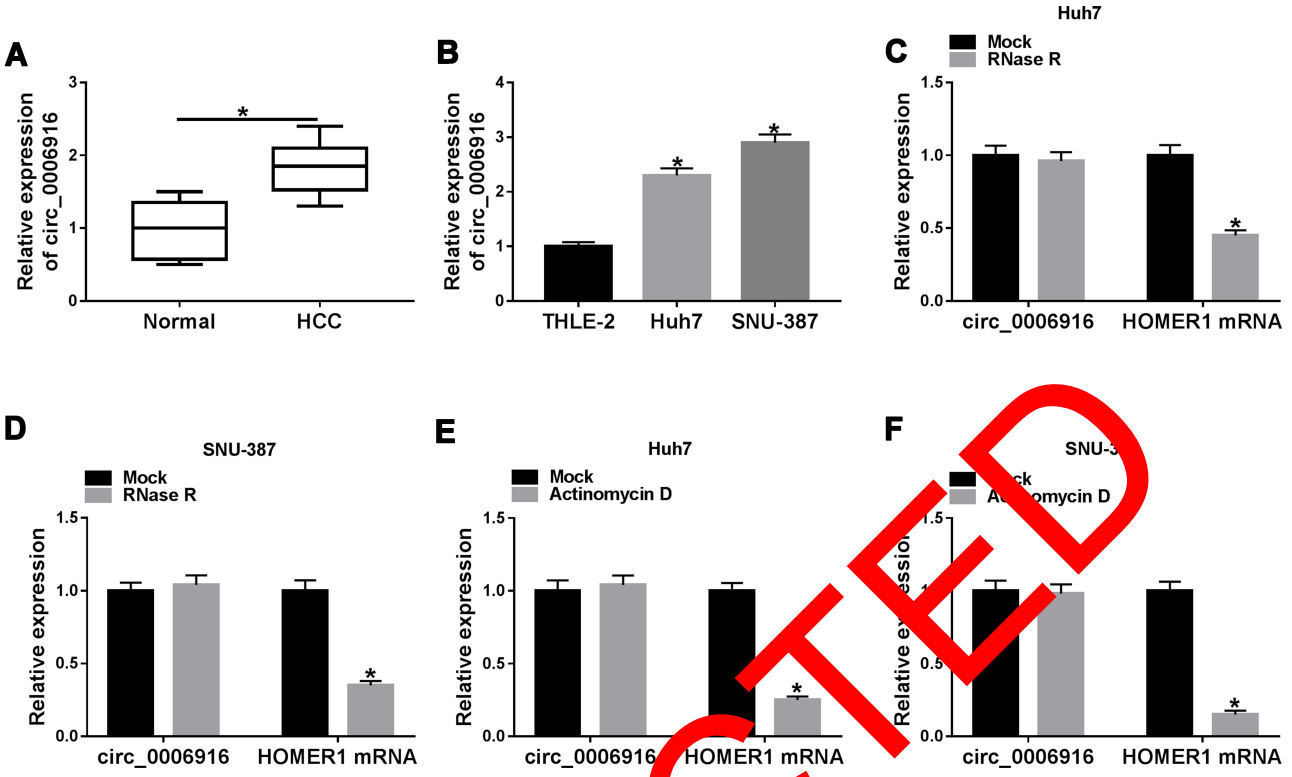

Figure 1 Circ_0006916 expression in HCC. (**A**) circ_0006916 level in HCC tissues (n = 30) and normal samples. (**B**) circ_0006916 abundance in Huh7, SNU-387 and THLE-2 cells. (**C** and **D**) circ_0006916 and *HOMER1* levels in Huh7 and SNU-387 cells were detected after treatment of RNase R. (**E** and **F**) circ_0006916 and *HOMER1* levels in Huh7 and SNU-387 cells were measured after treatment of Actinomycin D. *P<0.

stability of circ_0006916, circ_0006916 and corresponding linear HOMER1 levels were detected in cells after treatment of RNase R or Actinomycin D. As displayed in Figure 1C–F, circ_0006916 was more resistant to RNase R and Actinomycin D than the linear HOMER1. These results indicated that circ_0006916 was stably expressed in HCC, and the increased expression of circ_0006916 might be associated with HCC development.

circ_0006916 Knockdown Inhibits HCC Development in vitro

To analyze the function of circ_0006916 in HCC development, circ_0006916 expression was knocked down in Huh7 and SNU-387 cells using the siRNA targeting circ_0006916 (si-circ_0006916). The knockdown efficacy of si-circ_0006916 is confirmed in Figure 2A. Meanwhile, the introduction of si-circ_0006916 did not affect the abundance of the linear *HOMER1* (Figure 2B). The results of CCK8 and colony formation analyses displayed that circ_0006916 silence markedly decreased cell viability and colony ability (Figure 2C and D). Furthermore, the data of wound healing and transwell analyses displayed that circ_0006916 silence obviously inhibited cell migration and invasion (Figure 2E–G). Additionally, circ_0006916 interference caused cell cycle arrest at G0/G1 phase, revealed by the increased proportion of cells at G0/G1 phase and the reduced proportion of cells at S phase (Figure 2H). Besides, circ_0006916 silence evidently promoted cell apoptosis in Huh7 and SNU-387 cells (Figure 2I). Taken together, circ_0006916 knockdown repressed HCC cell progression.

miR-599 is Targeted via circ_0006916

To explore the regulatory network mediated via circ_0006916, the targeted miRNA was searched. miR-599 was one predicted target of circ_0006916. To confirm this prediction, we constructed the luciferase reporter vectors circ_0006916 WT and circ_0006916 MUT, and the targeted sequence is shown in Figure 3A. The data of dual-luciferase reporter analysis showed that miR-599 addition evidently decreased the luciferase activity of circ_0006916 WT, while it did not alter the luciferase activity of circ_0006916 MUT (Figure 3B and C). Furthermore, miR-599 expression was lower in HCC tissues than normal tissues (n = 30) (Figure 3D). And miR-599 expression was negatively associated with circ_0006916 level in HCC tissues (r = −0.6014, *P* =

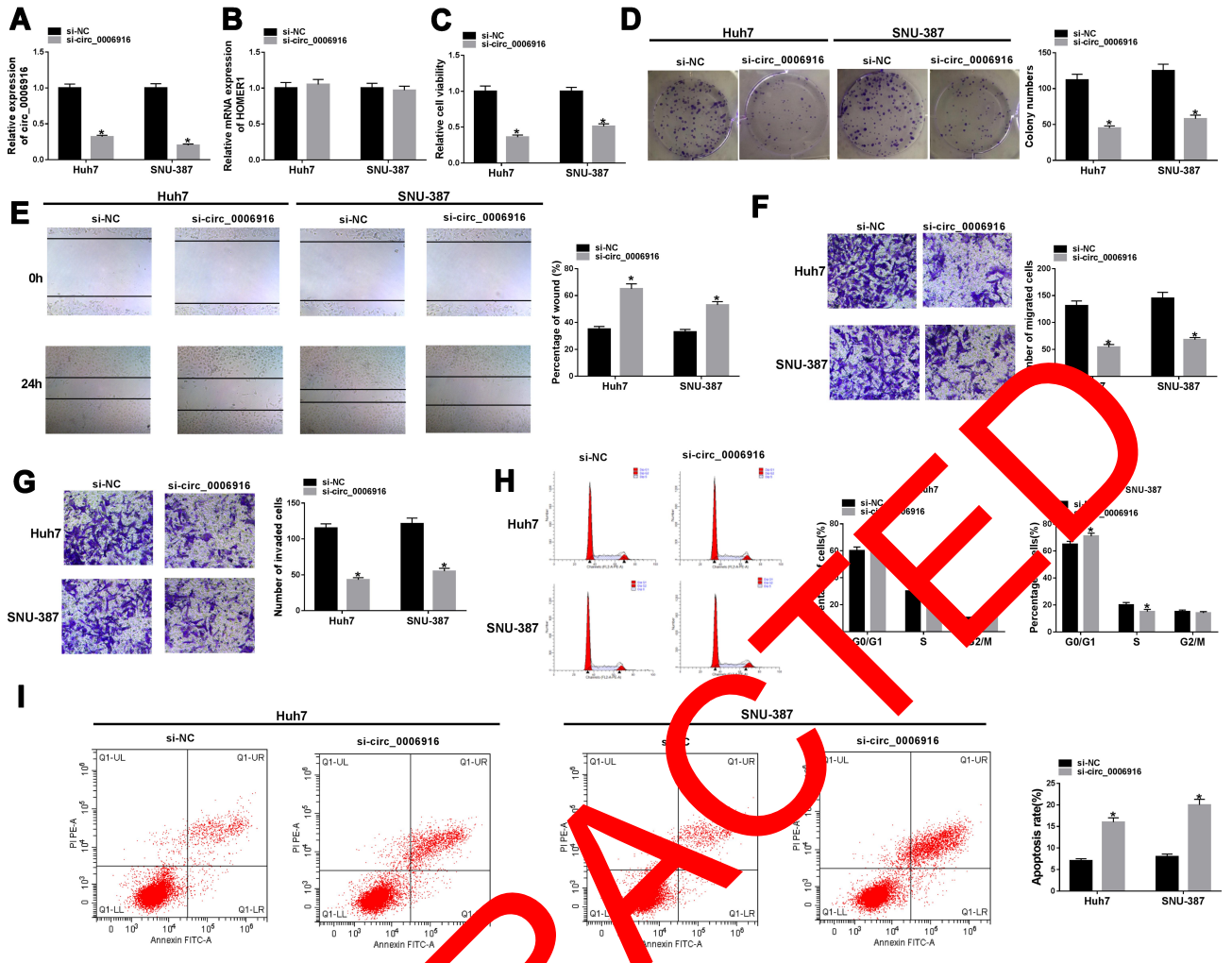

Figure 2 The impact of circ_0006916 on HCC cell pro[illegible] and *HOMER1* levels were detected in Huh7 and SNU-387 cells with transfection of si-NC or si-circ_0006916. Cell viability (**C**), colony f[illegible]ation (**D**)[illegible]ration and invasion (**E**–**G**), cycle distribution (**H**) and apoptosis (**I**) were examined in Huh7 and SNU-387 cells with transfection of si-NC or si-circ_00[illegible]16. *P<0.05.

0.0004) (Supplementary Fi[illegible]re 1A). In ad[illegible]ion, miR-599 level was significantly [illegible]ecrease[illegible] in Huh7 and SNU-387 cells in comparison to [illegible]LE[illegible] cells (Figure 3E). Besides, there were amou[illegible] circ_[illegible]06916 [illegible]d miR-599 enriched via Ago2 RI[illegible] (Figur[illegible]3F and [illegible]. These results suggested that miR-5[illegible] was ta[illegible]d via circ_0006916.

miR-599 Knoc[illegible]down Reverses the Influence of circ_0006916 Silence on HCC Development in vitro

To explore whether miR-599 was required for circ_0006916-mediated HCC development, Huh7 and SNU-387 cells were transfected with si-NC, si-circ _0006916, si-circ_0006916 + inhibitor NC or miR-599 inhibitor. The efficacy of miR-599 inhibitor is identified in Figure 4A. Moreover, miR-599 expression was evidently up-regulated via circ_0006916 knockdown, which was weakened via transfection of miR-599 inhibitor (Figure 4B). Moreover, miR-599 knockdown attenuated silence of circ_0006916-mediated inhibition of cell viability and colony ability (Figure 4C and D). In addition, miR-599 knockdown reversed interference of circ_0006916-mediated suppression of migration and invasion (Figure 4E–G). Besides, miR-599 down-regulation mitigated knockdown of circ_0006916-induced cycle arrest and apoptosis (Figure 4H–J). These results indicated that circ_0006916 silence repressed HCC cell progression via regulating miR-599.

SRSF2 is Targeted via miR-599

To further analyze the regulatory network involved in this study, the target of miR-599 was searched. *SRSF2* was

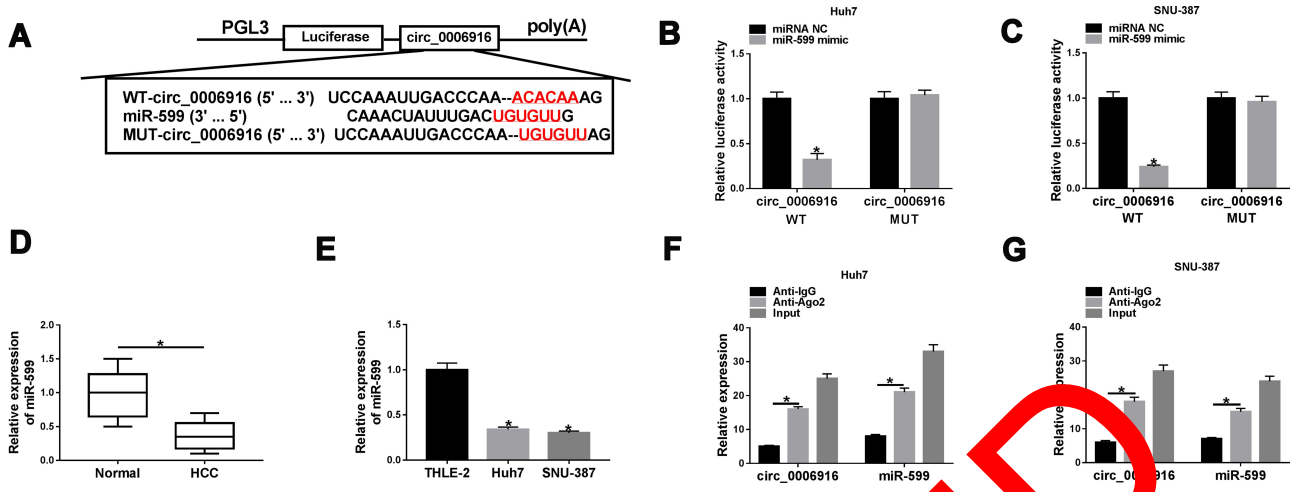

Figure 3 The association of circ_0006916 and miR-599. (**A**) The target sequence of circ_0006916 and miR-599. (**B** and **C**) Luciferase activity was detected in Huh7 and SNU-387 cells with transfection of circ_0006916 WT or circ_0006916 MUT and miR-599 mimic or miRNA NC. (**D**) miR-599 level in HCC tissue samples (n = 30) and normal samples. (**E**) miR-599 abundance in Huh7, SNU-387 and THLE-2 cells. (**F** and **G**) circ_0006916 and miR-599 levels were detected in Huh7 and SNU-387 cells after RIP. *P<0.05.

a candidate target, and the luciferase reporter vectors SRSF2-3′UTR WT and SRSF2-3′UTR MUT were constructed (Figure 5A). The data of dual-luciferase reporter analysis displayed that miR-599 overexpression remarkably reduced the luciferase activity of SRSF2-3′UTR WT, while it showed little impact on the luciferase activity of SRSF2-3′UTR MUT (Figure 5B and C). Moreover, RIP assay showed that miR-599 and *SRSF2* could be enriched in the same complex via Ago2 RIP (Figure 5D and E). Additionally, SRSF2 protein abundance was evidently elevated in HCC tissues and cells when compared to the corresponding normal tissues or cells (Figure 5F and G). And *SRSF2* abundance was negatively correlated with miR-599 level in HCC tissues (r = −0.4771, P = 0.0077) (Supplementary Figure 1). Besides, the influence of miR-599 on SRSF2 expression was investigated. The efficacy of SRSF2 overexpression vector is validated in Figure 5H. Furthermore, miR-599 overexpression evidently reduced SRSF2 protein expression, and this effect was attenuated via introduction of SRSF2 overexpression vector (Figure 5I). These results suggested that *SRSF2* was targeted via miR-599.

miR-599 Inhibits HCC Development via Targeting SRSF2

To analyze the function of miR-599 and whether it required *SRSF2*, Huh7 and SNU-387 cells were transfected with miRNA NC, miR-599 mimic, miR-599 mimic + pc-NC or pc-SRSF2. Moreover, miR-599 overexpression suppressed cell viability and colony ability in Huh7 and SNU-387 cells, which was mitigated via *SRSF2* up-regulation (Figure 6A and B). In addition, miR-599 up-regulation evidently reduced the abilities of migration and invasion, which was alleviated via *SRSF2* overexpression (Figure 6C–E). Furthermore, miR-599 overexpression facilitated cell cycle arrest at G0/G1 phase and apoptosis, and this effect was weakened via *SRSF2* overexpression (Figure 6F–H). These data suggested that miR-599 repressed HCC cell progression via regulating *SRSF2*.

circ_0006916 Knockdown Decreases SRSF2 Expression via miR-599

To explore how and whether circ_0006916 could regulate SRSF2, Huh7 and SNU-387 cells were transfected with si-NC, si-circ_0006916, si-circ_0006916 + pc-NC or pc-SRSF2. As displayed in Figure 7A, SRSF2 abundance was evidently decreased via circ_0006916 knockdown, which was restored via transfection of SRSF2 overexpression vector. Moreover, Huh7 and SNU-387 cells were transfected with si-NC, si-circ_0006916, si-circ_0006916 + inhibitor NC or miR-599 inhibitor. Results showed that miR-599 knockdown mitigated the suppressive effect of circ_0006916 silence on SRSF2 expression in Huh7 and SNU-387 cells (Figure 7B). These results showed that circ_0006916 could regulate SRSF2 expression via modulating miR-599.

circ_0006916 Silence Decreases Xenograft Tumor Growth

To explore the function of circ_0006916 in HCC development in vivo, SNU-387 cells with stable transfection of sh-

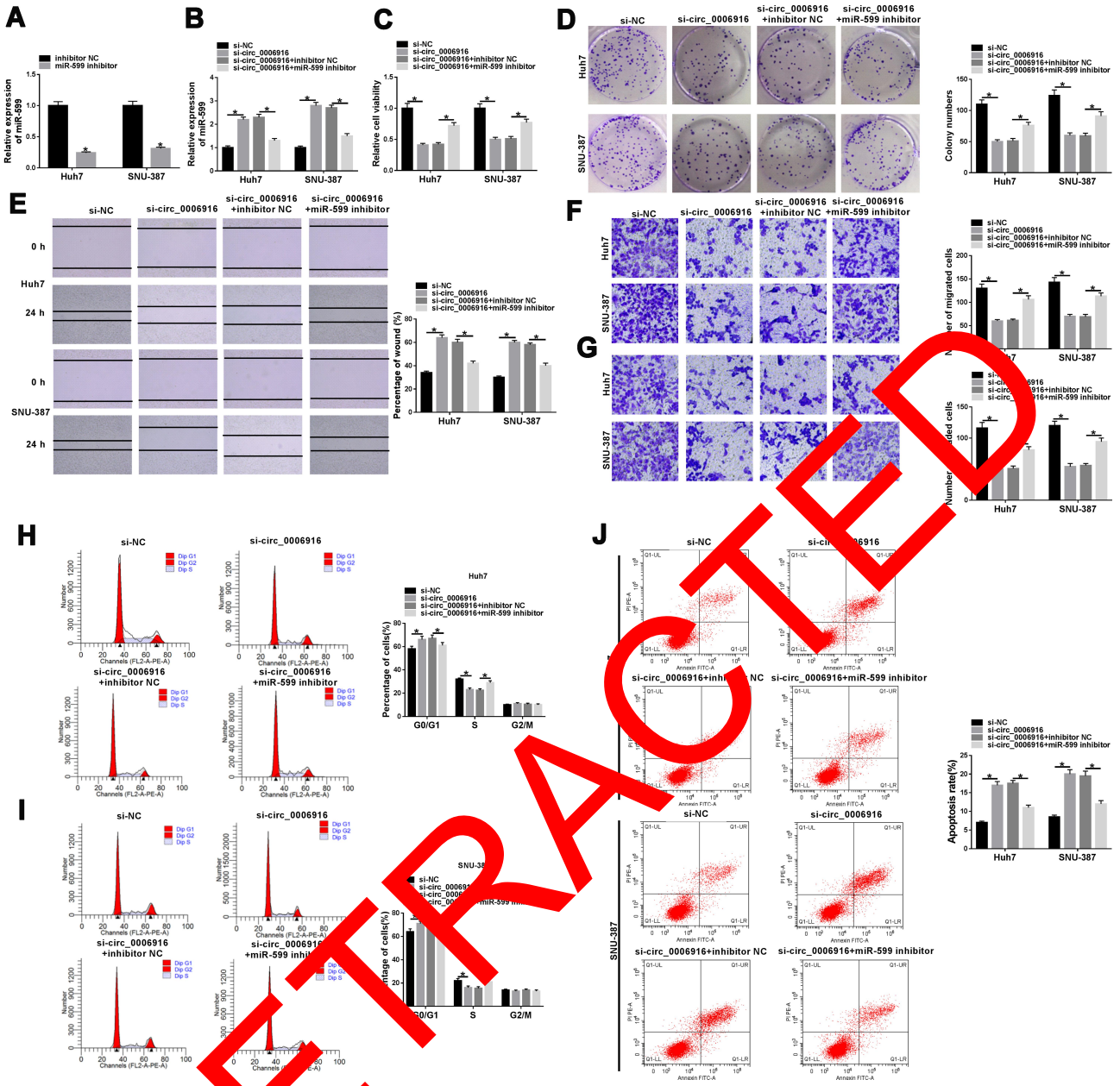

Figure 4 The effect of [illegible]9 on ci[illegible]0006916-[illegible]diated HCC cell progression. (**A**) miR-599 expression was detected in Huh7 and SNU-387 cells with transfection of inhibitor NC or mi[illegible]9 inhib[illegible]r. miR-5[illegible]bu[illegible]nce (**B**), cell viability (**C**), colony formation (**D**), migration and invasion (**E**–**G**), cycle distribution (**H** and **I**) and apoptosis (**J**) were measur[illegible]n Huh7 ar[illegible]SNU-387 ce[illegible]with transfection of si-NC, si-circ_0006916, si-circ_0006916 + inhibitor NC or miR-599 inhibitor. *P<0.05.

NC or sh-circ_0[illegible]6916 were inoculated into mice to establish the xenograft mo[illegible]el. The mice were divided into sh-NC or sh-circ_0006916 group (n = 6). After 28 days, the tumor volume and weight were evidently reduced in sh-circ_0006916 group compared with sh-NC group (Figure 8A and B). Moreover, circ_0006916, miR-599 and SRSF2 abundances were detected in the tumor tissues. As displayed in Figure 8C–E, circ_0006916 and SRSF2 abundances were evidently reduced and miR-599 expression was enhanced in sh-circ_0006916 group in comparison to sh-NC group. These results indicated circ_0006916 down-regulation inhibited HCC development in vivo.

Discussion

HCC is the major liver cancer with high incidence and mortality.[28] Moreover, the overall survival of HCC patients is lower than 18%.[29] CircRNAs are implicated in the progression of liver diseases including HCC via regulating various cell events.[30] A previous study suggested that circ_0006916 played an important role in

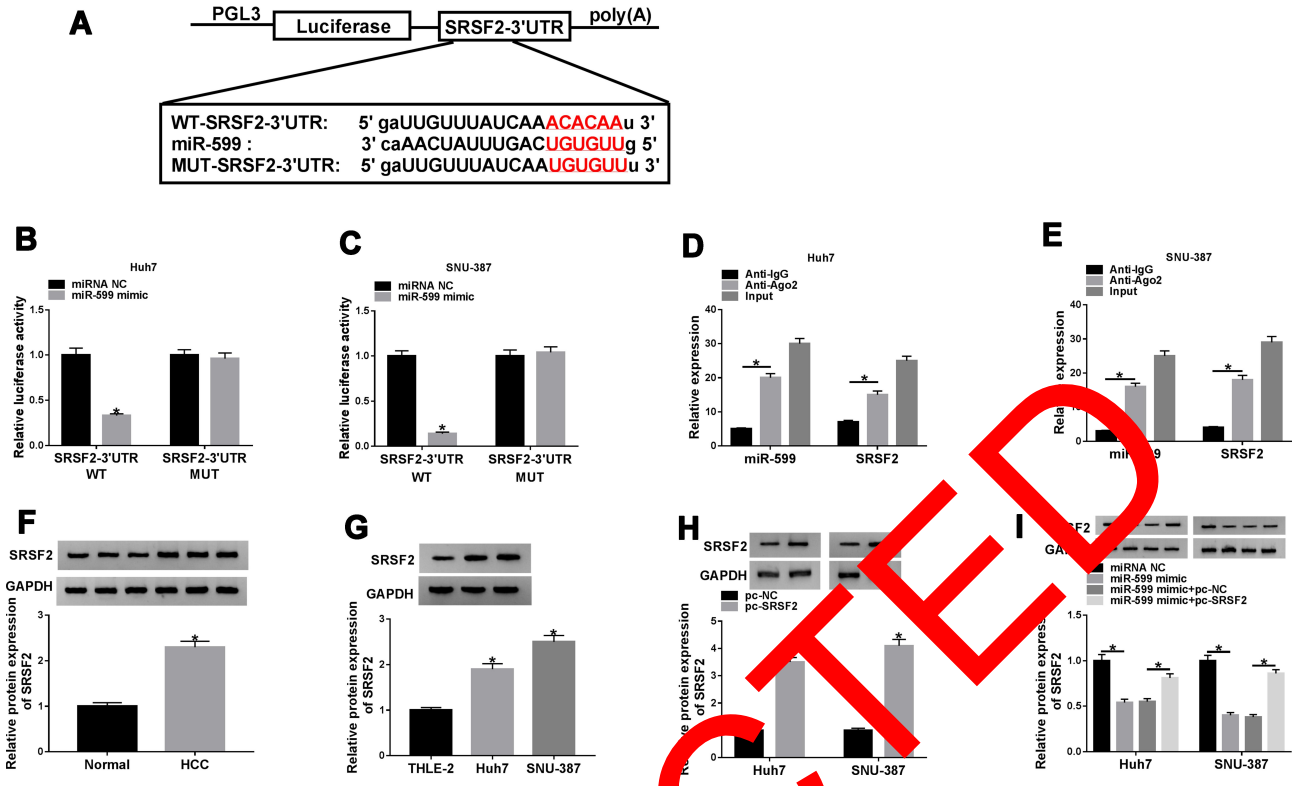

Figure 5 The relationship of miR-599 and *SRSF2*. (**A**) The target sequence of miR-599 and *SRSF2*. (**B** and) Luciferase activity was measured in Huh7 and SNU-387 cells with transfection of SRSF2-3′UTR WT or SRSF2-3′UTR MUT and miR-599 mimic or miR- NC. (**D** and) miR-599 and *SRSF2* abundances were examined in Huh7 and SNU-387 cells after RIP. (**F**) SRSF2 expression in HCC tissues and normal ples. (**G**) SRS in Huh7, SNU-387 and THLE-2 cells. (**H**) SRSF2 abundance was detected in Huh7 and SNU-387 cells with transfection of pc-NC or pc-SRS (**I**) level was detected in cells with transfection of miRNA NC, miR-599 mimic, miR-599 mimic + pc-NC or pc-SRSF2. **P*<0.05.

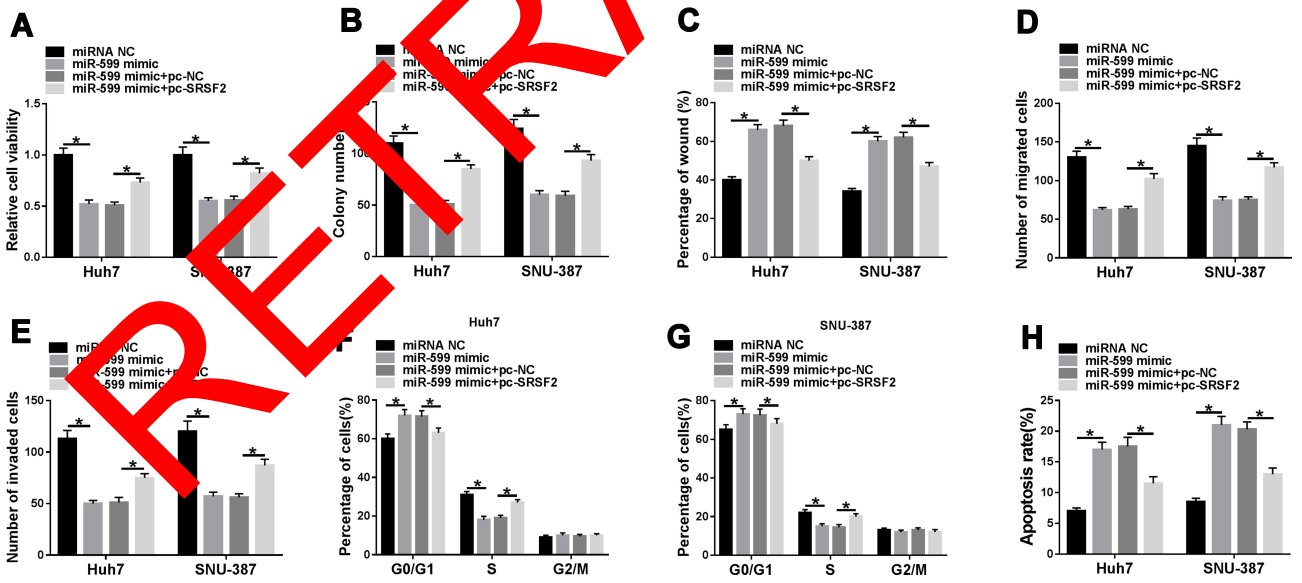

Figure 6 The influence of miR-599 and *SRSF2* on HCC cell progression. Cell viability (**A**), colony formation (**B**), migration and invasion (**C**–**E**), cycle distribution (**F** and **G**) and apoptosis (**H**) were examined in Huh7 and SNU-387 cells with transfection of miRNA NC, miR-599 mimic, miR-599 mimic + pc-NC or pc-SRSF2. **P*<0.05.

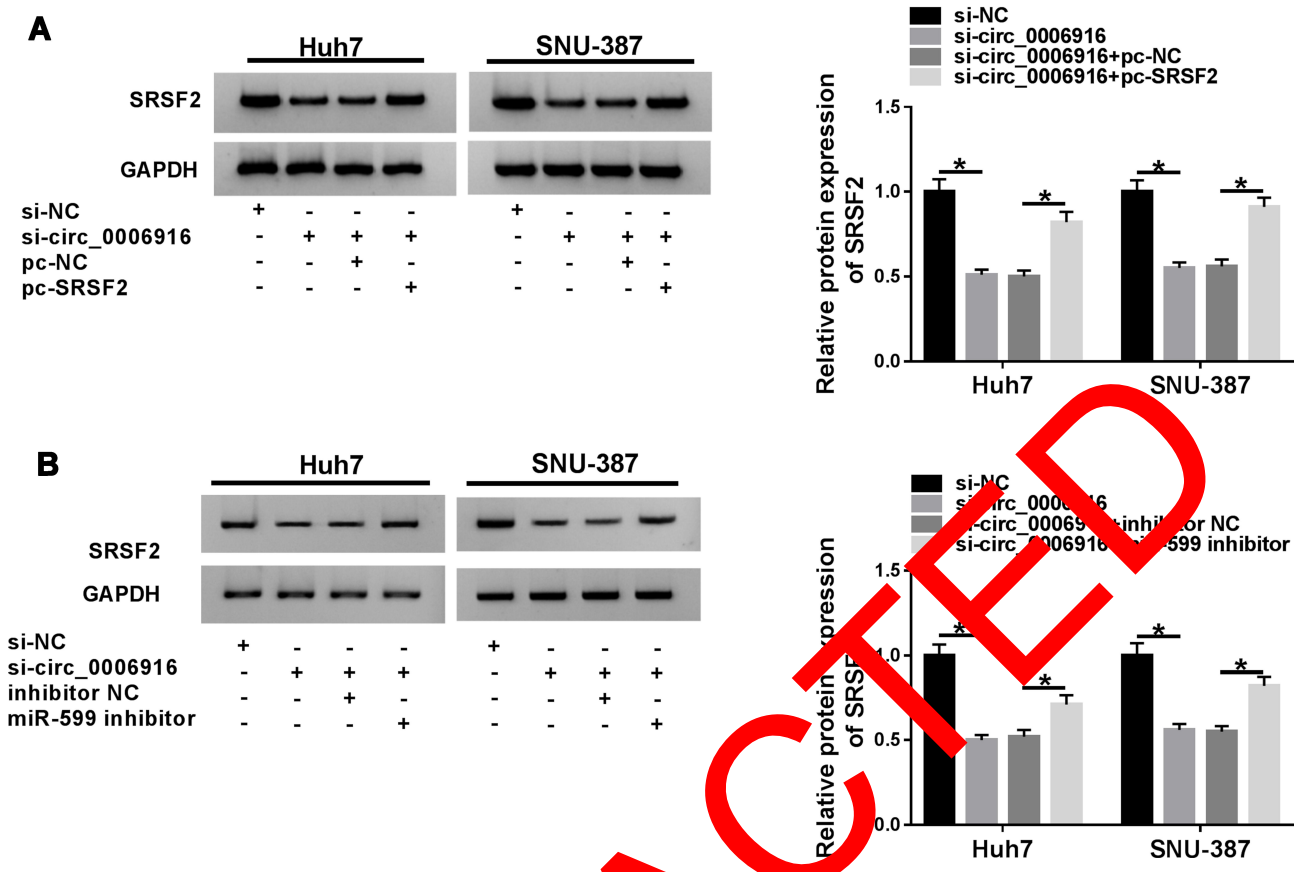

Figure 7 The influence of miR-599 and circ_0006916 on SRSF2 abundance. (**A**) SRSF2 protein level was detected in Huh7 and SNU-387 cells with transfection of si-NC, si-circ_0006916, si-circ_0006916 + pc-NC or pc-SRSF2. (**B**) SRSF2 protein expression was measured in Huh7 and SNU-387 cells with transfection of si-NC, si-circ_0006916, si-circ_0006916 + inhibitor NC or miR-599 inhibitor. *P<0.05.

HCC development.[15] In this study, we found that circ_0006916 could repress HCC development. Moreover, we were the first time to validate it was associated with circ_0006916/miR-599/*SRSF2* network in HCC.

In this research, we found circ_0006916 abundance was elevated in HCC which was also consistent with former reports.[14,15] Moreover, by treatment of RNase R and Actinomycin D, we found that circ_0006916 was stably expressed in HCC cells. To explore the potential role of circ_0006916, we performed the loss-of-function experiments, and found that circ_0006916 interference restrained HCC development via reducing cell viability, colony ability, migration and invasion and increasing cycle arrest and apoptosis, which was also like that in a previous report.[15] Nevertheless, the role of circ_0006916 in HCC was opposite to that in lung cancer as a previous report.[12] We hypothesized that the differences of circ_0006916 expression and function between the two cancers might be caused via the different tumor microenvironment. Furthermore, to explore the function of circ_0006916 in vivo, we established the xenograft model, and validated the anti-HCC role of circ_0006916 interference.

The regulatory network of circRNA/miRNA/mRNA is a major mechanism for circRNA in a competing endogenous RNA (ceRNA) manner.[31] A previous study has confirmed the circ_0006916/miR-1322/*CXCL6* regulatory network in HCC.[15] Our study wanted to explore an additional network. Here we used dual-luciferase reporter and RIP analyses to identify miR-599 was targeted via circ_0006916. The decreased miR-599 was detected in HCC tissues and cells, indicating the decreased miR-599 might be associated with the malignancy of HCC. Moreover, we found that miR-599 overexpression using the miR-599 mimic repressed HCC development via decreasing cell viability, colony formation, migration and invasion. These results implied that miR-599 played a suppressive role in HCC, which was like that in a previous report.[19] This is also consistent with the role of miR-599 in other cancers, including esophageal

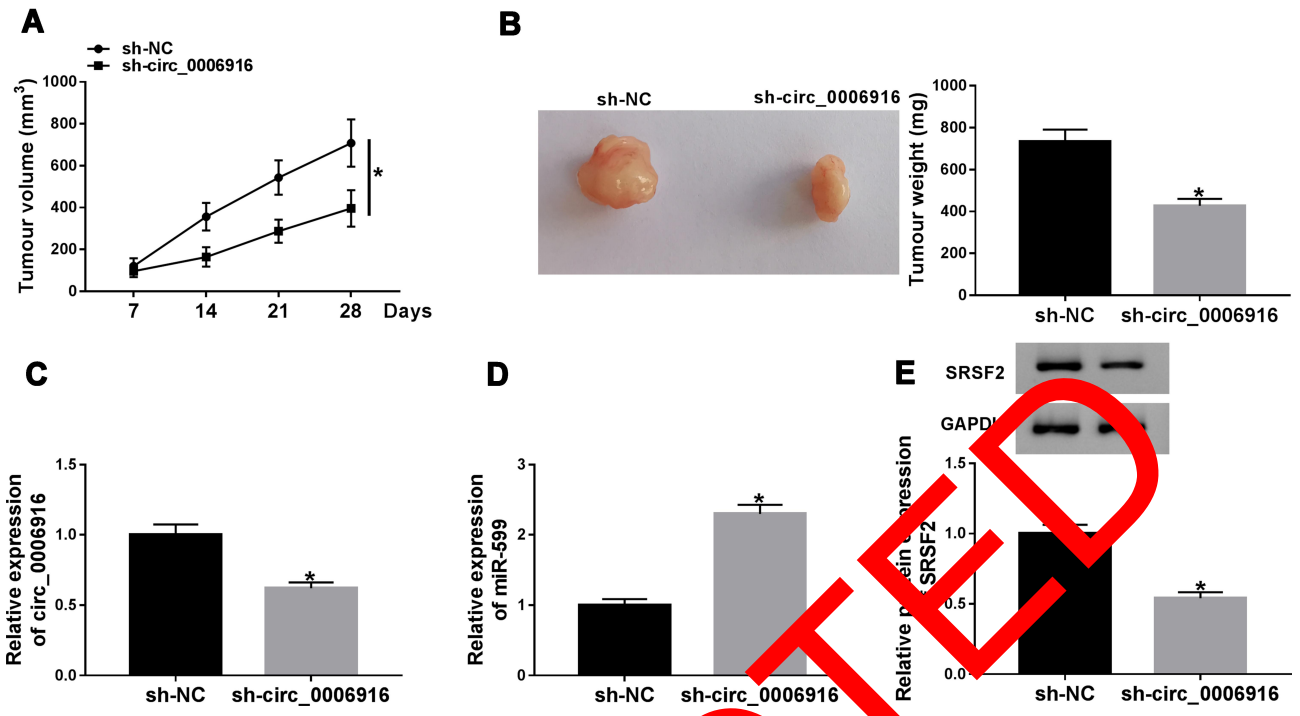

Figure 8 The impact of circ_0006916 on HCC cell growth in vivo. (**A**) Tumor volume was measured every 7 days. (**B**) Tumor weight was examined. (**C–E**) circ_0006916, miR-599 and SRSF2 abundances were examined in tumor tissues. *P<0.05.

carcinoma, gastric cancer, breast cancer, glioma and anaplastic thyroid cancer.[32–36] In addition, we found that miR-599 knockdown attenuated the effect of circ_0006916 silence on HCC development, indicating circ_0006916 could regulate HCC development via controlling miR-599.

Next, we identified miR-599 could target *SRSF2*. Here we found that *SRSF2* expression was enhanced in HCC, which was also in agreement with a previous study.[20] Luo et al reported that *SRSF2* could contribute to HCC cell proliferation.[21] Furthermore, Ma et al showed that *SRSF2* down-regulation repressed cell proliferation and caused G1 phase arrest in HCC.[37] These reports suggested *SRSF2* played a carcinogenic role in HCC. Moreover, we found that *SRSF2* overexpression attenuated the suppressive effect of miR-599 on HCC development. In addition, our results showed that circ_0006916 could regulate *SRSF2* via competitively binding to miR-599. Hence, we concluded that circ_0006916 could regulate HCC development via modulating miR-599/*SRSF2* axis.

In conclusion, circ_0006916 silence repressed HCC development, possibly via regulating miR-599 and *SRSF2*. This research proposed a novel insight into the pathogenesis of HCC, and indicated circ_0006916 could be used as a target for the treatment of HCC.

Highlights

1. circ_0006916 abundance is elevated in hepatocellular carcinoma.
2. circ_0006916 knockdown restrains cell viability, colony formation, migration and invasion.
3. circ_0006916 knockdown facilitates cell apoptosis.
4. circ_0006916 could modulate *SRSF2* via sponging miR-599.
5. circ_0006916 knockdown decreases xenograft tumor growth.

Ethics Approval

This work was approved by Henan Province Medical Science and Technology (LHGJ20190515)

Disclosure

The authors declare that they have no financial or non-financial conflicts of interest for this work.

References

1. Forner A, Reig M, Bruix J. Hepatocellular carcinoma. *Lancet*. 2018;391(10127):1301–1314. doi:10.1016/S0140-6736(18)30010-2
2. Yang JD, Hainaut P, Gores GJ, Amadou A, Plymoth A, Roberts LR. A global view of hepatocellular carcinoma: trends, risk, prevention and management. *Nat Rev Gastroenterol Hepatol*. 2019;16(10):589–604. doi:10.1038/s41575-019-0186-y

3. Tabrizian P, Jibara G, Shrager B, Schwartz M, Roayaie S. Recurrence of hepatocellular cancer after resection: patterns, treatments, and prognosis. *Ann Surg*. 2015;261(5):947–955. doi:10.1097/SLA.0000000000000710
4. Klingenberg M, Matsuda A, Diederichs S, Patel T. Non-coding RNA in hepatocellular carcinoma: mechanisms, biomarkers and therapeutic targets. *J Hepatol*. 2017;67(3):603–618. doi:10.1016/j.jhep.2017.04.009
5. Qiu L, Xu H, Ji M, et al. Circular RNAs in hepatocellular carcinoma: biomarkers, functions and mechanisms. *Life Sci*. 2019;231:116660. doi:10.1016/j.lfs.2019.116660
6. Sun X, Ge X, Xu Z, Chen D. Identification of circular RNA-microRNA-messenger RNA regulatory network in hepatocellular carcinoma by integrated analysis. *J Gastroenterol Hepatol*. 2020;35(1):157–164. doi:10.1111/jgh.14762
7. Li Z, Liu Y, Yan J, et al. Circular RNA hsa_circ_0056836 functions an oncogenic gene in hepatocellular carcinoma through modulating miR-766-3p/FOSL2 axis. *Aging (Albany NY)*. 2020;12(3):2485–2497. doi:10.18632/aging.102756
8. Pu J, Wang J, Li W, et al. hsa_circ_0000092 promotes hepatocellular carcinoma progression through up-regulating HN1 expression by binding to microRNA-338-3p. *J Cell Mol Med*. 2020. doi:10.1111/jcmm.15010
9. Su X, Su J, He H, Zhan Y, Liu H. Hsa_circ_0070269 inhibits hepatocellular carcinoma progression through modulating miR-182/NPTX1 axis. *Biomed Pharmacother*. 2019;120:109497. doi:10.1016/j.biopha.2019.109497
10. Liu Z, Yu Y, Huang Z, et al. CircRNA-5692 inhibits the progression of hepatocellular carcinoma by sponging miR-328-5p to enhance DAB2IP expression. *Cell Death Dis*. 2019;10(12):900. doi:10.1038/s41419-019-2089-9
11. Jiang L, Zhao L, Bi J, et al. Glycolysis gene expression profilings screen for prognostic risk signature of hepatocellular carcinoma. *Aging (Albany NY)*. 2019;11(23):10861–10882.
12. Dai X, Zhang N, Cheng Y, et al. RNA-binding protein trinucleotide repeat-containing 6A regulates the formation of circular RNA circ0006916, with important functions in lung cancer cell. *Carcinogenesis*. 2018;39(8):981–992. doi:10.1093/carcin/bgy061
13. Li J, Sun Q, Zhu S, et al. Knockdown of circHomer1 ameliorates METH-induced neuronal injury through inhibiting Bnc3 expression. *Neurosci Lett*. 2020;732:135050. doi:10.1016/j.neulet.2020.135050
14. Xu L, Feng X, Hao X, et al. CircSETD3 (Hsa_circ_0005075) acts as a sponge for microRNA-421 inhibiting hepatocellular carcinoma growth. *J Exp Clin Cancer Res*. 2019;38(1):98. doi:10.1186/s13046-019-1041-2
15. Zhao M, Dong G, Meng Q, Lin S, Liu C. CircHOMER1 enhances the inhibition of miR-1322 on CXCL6 to regulate cell growth and aggressiveness of hepatocellular carcinoma cells. *J Cell Biochem*. 2020.
16. Xu X, Tao Y, Shan L, et al. The role of microRNAs in hepatocellular carcinoma. *J Cancer*. 2016;7(9):1357–1369.
17. Ba Y, Liu Y, Li C, Zhu X, Xin W. HIPK3 promotes growth and metastasis of esophageal squamous cell carcinoma via regulation of miR-599/c-MYC axis. *Onco Targets Ther*. 2020;13:1967–1978. doi:10.2147/OTT.S217127
18. Zhang X, Li BF, Luo L, et al. LncRNA DANCR-miR-758-3p-PAX6 molecular network regulates apoptosis and autophagy of breast cancer cells. *Cancer Manag Res*. 2020;12:4073–4084. doi:10.2147/CMAR.S254069
19. Tian J, Hu X, Gao W, et al. Identification a novel tumor-suppressive hsa-miR-599 regulates cells proliferation, migration and invasion by targeting oncogenic MYC in hepatocellular carcinoma. *Am J Transl Res*. 2016;8(6):2575–2584.
20. Wang P, Guo L, Li K, et al. Serine/arginine rich splicing factor 2 expression and clinic pathological features indicating a prognostic factor in human hepatocellular carcinoma patients. *Cancer Biomark*. 2018;21(3):681–687. doi:10.3233/CBM-170770
21. Luo C, Cheng Y, Liu Y, et al. SRSF2 regulates alternative splicing to drive hepatocellular carcinoma development. *Cancer Res*. 2017;77(5):1168–1178.
22. Chomczynski P, Sacchi N. The single-step method of RNA isolation by acid guanidinium thiocyanate-phenol-chloroform extraction: twenty-something years on. *Nat Protoc*. 2006;1(2):581–585. doi:10.1038/nprot.2006.83
23. Livak KJ, Schmittgen TD. Analysis of relative gene expression data using real-time quantitative PCR and the 2(-Delta Delta C (T)) method. *Methods*. 2001;25(4):402–408. doi:10.1006/meth.2001.1262
24. Peng QS, Cheng YN, Zhang WB, Fan H, Mao QH, Xu P. circRNA_0000140 suppresses oral squamous cell carcinoma growth and metastasis by targeting miR-31 to inhibit hippo signaling pathway. *Cell Death Dis*. 2020;11(2):112. doi:10.1038/s41419-020-2273-y
25. Jia Q, Ye L, Xu S, et al. Circular RNA 000723 regulates the progression of breast cancer through miR-335-5p/SIX1 axis. *Thorac Cancer*. 2020;11(3):619–630. doi:10.1111/1759-7714.13306
26. Dudekula DB, Panda AC, Grammatikakis I, De S, Abdelmohsen K, Gorospe M. CircInteractome: a web tool for exploring circular RNAs and their interacting proteins and microRNAs. *RNA Biol*. 2016;13(1):34–42. doi:10.1080/15476286.2015.1128065
27. Li JH, Liu S, Zhou H, Qu LH, Yang JH. starBase v2.0: decoding miRNA-ceRNA, miRNA-ncRNA and protein-RNA interaction networks from large-scale CLIP-Seq data. *Nucleic Acids Res*. 2014;42(Database issue):D92–7. doi:10.1093/nar/gkt1248
28. Ryerson AB, Eheman CR, Altekruse SF, et al. Annual report to the nation on the status of cancer, 1975–2012, featuring the increasing incidence of liver cancer. *Cancer*. 2016;122(9):1312–1337. doi:10.1002/cncr.29936
29. Villanueva A. Hepatocellular carcinoma. *N Engl J Med*. 2019;380(15):1450–1462. doi:10.1056/NEJMra1713263
30. Chien Y, Tsai PH, Lai YH, et al. CircularRNA as novel biomarkers in diseases. *J Chin Med Assoc*. 2020;83(1):15–17.
31. Wu J, Liu S, Xiang Y, Qu X, Xie Y, Zhang X. Bioinformatic analysis of circular RNA-associated ceRNA network associated with hepatocellular carcinoma. *Biomed Res Int*. 2019;2019:8308694. doi:10.1155/2019/8308694
32. Wang C, Tang D, Wang H, et al. Circular RNA hsa_circ_0030018 acts as a sponge of miR-599 to aggravate esophageal carcinoma progression by regulating ENAH expression. *J Cell Biochem*. 2019.
33. Cheng Y, Su Y, Wang S, et al. Identification of circRNA-lncRNA-miRNA-mRNA competitive endogenous RNA network as novel prognostic markers for acute myeloid leukemia. *Genes (Basel)*. 2020;11(8). doi:10.3390/genes11080868.
34. Wang Y, Sui Y, Zhu Q, Sui X. Hsa-miR-599 suppresses the migration and invasion by targeting BRD4 in breast cancer. *Oncol Lett*. 2017;14(3):3455–3462. doi:10.3892/ol.2017.6651
35. Jiang Y, Wang X, Zhang J, Lai R. MicroRNA-599 suppresses glioma progression by targeting RAB27B. *Oncol Lett*. 2018;16(1):1243–1252.
36. Bi JW, Zou YL, Qian JT, Chen WB. MiR-599 serves a suppressive role in anaplastic thyroid cancer by activating the T-cell intracellular antigen. *Exp Ther Med*. 2019;18(4):2413–2420.
37. Ma K, He Y, Zhang H, et al. DNA methylation-regulated miR-193a-3p dictates resistance of hepatocellular carcinoma to 5-fluorouracil via repression of SRSF2 expression. *J Biol Chem*. 2012;287(8):5639–5649. doi:10.1074/jbc.M111.291229